Induced gravitational waves via warm natural inflation

Miguel Correa,[1,*] Mayukh R. Gangopadhyay,[2,†] Nur Jaman,[3,‡] and Grant J. Mathews[1,§]

[1]Center for Astrophysics, Department of Physics and Astronomy, University of Notre Dame, Notre Dame, Indiana 46556, USA

[2]Centre For Cosmology and Science Popularization (CCSP), SGT University, Gurugram, Delhi- NCR, Haryana—122505, India

[3]Department of Physical Sciences, Indian Institute of Science Education and Research Kolkata, Mohanpur—741 246, WB, India

(Received 24 June 2023; accepted 14 February 2024; published 26 March 2024)

We analyze the spectrum of gravitational waves generated by the induced spectrum of tensor fluctuation during warm natural inflation. In our previous work, it has been demonstrated that an epoch of warm natural inflation can lead to cosmologically relevant dark matter production in the form of primordial black holes. Here, we show that models that solve the dark-matter production also produce a contribution to the cosmic gravitational wave background that satisfies current constraints from pulsar timing and big bang nucleosynthesis. More importantly, this gravitational wave background may be observable in the next generation of space-based and ground-based gravitational wave interferometers.

DOI: 10.1103/PhysRevD.109.063539

I. INTRODUCTION

In our previous paper [1], we investigated the intriguing properties of a cosmic inflationary paradigm [2–5] in which the inflaton effective potential is based on the natural potential [6], and where there exists a coupling between the inflaton field and matter fields such that matter is continuously produced during the inflationary epoch (Warm Inflation [7–19]). This so-called "warm natural inflation" (WNI) paradigm was first studied by [20,21] and more recently by [22–24]. In our study [1], we discovered that the model remarkably satisfies several observational and theoretical constraints. Firstly, it yields a spectral index and a ratio of the tensor-to-scalar power spectra that agree with constraints from the Planck mission [25,26] and BICEP/Keck [27,28]. Secondly, WNI allows for inflation to be in a sub-Planckian regime within the effective field theory framework. We found that it is consistent with the previously mentioned constraints for a symmetry-breaking scale of $f = 0.8$ with cubic dissipation ($\Gamma \propto T^3$). Recently, [23] also confirmed our results by finding it is consistent for $f_{\rm min} = 0.8$ in the parameter space. However, our most important finding is that WNI naturally leads to the significant generation of primordial black holes (PBHs).

The possibility of black hole formation in the early Universe has been a subject of consideration for decades [29–31]. Furthermore, it is known that if the mass of PBHs falls within an appropriate range permitted by observations, they could potentially explain the entirety of the inferred dark matter in the Universe [32–35]. Reference [36] demonstrated that warm inflation could produce sufficient enhancement in the scalar power spectrum to give rise to PBHs. Notably, WNI generates PBHs in significant quantities and within the correct mass range to account for a substantial fraction, if not all, of the observed dark matter content in the Universe.

As additional motivation, it has been pointed out [37] that a number of observational dilemmas can be understood if there is a significant population of PBHs. Among them, in a PBH-ΛCDM cosmology, the PBH dark matter mini halos can collapse earlier than those comprised of standard collisionless cold dark matter. This allows baryons to cool and form stars and galaxies at very high redshift. This is consistent with recent JWST observations [38] of bright galaxies at very high redshift ($z \sim 13$). The PBHs can also collect to provide seeds for supermassive black hole formation and thereby account for the DM-halo host-galaxy central-black-hole connection as manifested in the $M_{BH} - \sigma$ relation. They may also account [37] for the x-ray and infrared backgrounds and the early formation of the supermassive black holes powering quasars at $z > 7$.

However, one signature we did not consider in our previous study [1] was the possible spectrum of gravitational waves (GWs) associated with primordial black-hole production. The purpose of the present work, therefore, is to examine this constraint in the context of WNI models that can account for the cosmic dark matter content. As we will see, WNI has the capability to generate a GW spectrum that could be detectable by several future detectors.

*mcorrea2@nd.edu
†mayukh_ccsp@sgtuniversity.org
‡nurjaman.pdf@iiserkol.ac.in
§gmathews@nd.edu

There are two sources of primordial GWs that one needs to consider. First, are the quantum tensor perturbations generated during inflation: These are the primary GWs. Secondly are the classical GWs generated by the enhanced density perturbation. These are the secondary or induced GWs. In the language of perturbation theory, at linear order, the scalar and tensor modes evolve independently. In the second-order of perturbation, the scalar and tensor modes couple together. The scalar perturbation can then source the secondary tensor mode and thereby produce induced gravitational waves (IGWs) [39–44,44–46].

Usually, the second-order GWs are suppressed with respect to the first-order by a factor of the square of the scalar spectrum [39]. However, they can become significant and even exceed the first-order GWs for an enhanced primordial scalar power spectrum, such as in the case of PBH formation [40,47,48]. Indeed, it has been shown in the literature [41] that the second-order tensor mode dominates over the first-order if the tensor to scalar ratio is $r < 10^{-6}$. The induced gravitational wave production in the case of warm inflation has been studied previously in [49–52]. Here, we specifically consider GW production in warm natural inflation.

This paper is structured as follows: We briefly review the WNI dynamics in Sec. II. The modeling of GWs and a semianalytical calculation of the GW spectrum is given in Sec. III. We present our findings and compare the calculated spectrum to present and future detection sensitivities in Sec. IV. We provide discussion and conclusions in Sec. V.

II. WARM INFLATIONARY DYNAMICS

In a homogeneous and isotropic background, the dynamics of the inflaton field $\phi(t)$ within warm inflation are governed by the following equations:

$$\ddot{\phi} + 3H(1+Q)\dot{\phi} + V_{,\phi} = 0, \tag{1}$$

$$\dot{\rho}_R + 4H\rho_R = 3HQ\dot{\phi}^2, \tag{2}$$

$$3H^2M_{\rm Pl}^2 = (\rho_\phi + \rho_R), \tag{3}$$

where over-dots represent derivatives with respect to cosmic time t, $V_{,\phi} \equiv \partial V/\partial\phi$, ρ_r is the radiation energy density, and $Q \equiv \Gamma/3H$, where Γ is the dissipation coefficient providing the source for the radiation bath. The last equation is the Friedmann equation satisfied by the Hubble parameter H.

During inflation, the potential energy dominates over both the kinetic term and the radiation energy density, i.e.,

$$V(\phi) \gg \left\{\frac{1}{2}\dot{\phi}^2, \rho_r\right\}. \tag{4}$$

Also, the inflaton field amplitude should not change too quickly ($\ddot{\phi} < 3H\dot{\phi}$). Moreover, the condition of an accelerating scale factor ($\ddot{a} > 0$) then leads to the slow-roll condition for WI such that

$$3H(1+Q) \approx -V_{,\phi}, \tag{5}$$

and

$$-\frac{d\ln H}{dN} = \frac{\epsilon_\phi}{1+Q} \ll 1, \tag{6}$$

$$-\frac{d\ln V_{,\phi}}{dN} = \frac{\eta_\phi}{1+Q} \ll 1, \tag{7}$$

where $\epsilon_\phi = (M_{\rm Pl}^2/2)(V_{,\phi}/V)^2$ and $\eta_\phi = M_{\rm Pl}^2(V_{,\phi\phi}/V)$ are the usual cold inflationary (CI) slow-roll parameters. The quantity $N = \ln a$, with a the scale factor, denotes the number of e folds of inflation. Under the slow-roll approximation, the warm inflationary dynamics are then governed by the following:

$$3H(1+Q)\dot{\phi} \approx V_{,\phi}, \tag{8}$$

$$4\rho_r \approx 3Q\dot{\phi}^2, \tag{9}$$

$$3H^2M_{\rm Pl}^2 \approx V, \tag{10}$$

where the radiation energy density can also be written in terms of the temperature T, since $\rho_r = (\pi^2/30)g_*T^4$.

For our studies of warm inflation [1], we have adopted cubic dissipation $\Gamma = CT^3$ with C a constant of dimension $M_{\rm Pl}^{-2}$. The dynamical equation of inflation with respect to the number of e folds can be found in our earlier work [1].

The power spectrum for curvature and tensor perturbations in the case of warm inflation with a cubic dissipation coefficient are, respectively, given by (see Ref. [53] and references therein):

$$\mathcal{P}_R = \left(\frac{H^2}{2\pi\dot{\phi}}\right)^2\left(1+\frac{T}{H}F(Q)\right)G(Q), \tag{11}$$

$$\mathcal{P}_T = 2H^2/(\pi^2M_{\rm Pl}^2), \tag{12}$$

with

$$F(Q) \approx \frac{2\pi\sqrt{3}Q}{\sqrt{3+4\pi Q}}, \tag{13}$$

and

$$G(Q) = 1 + 4.981Q^{1.946} + 0.127Q^{4.330}, \tag{14}$$

where the $G(Q)$ approximates an exact numerical calculation of the effect of the coupling between the inflating fluctuations and radiation [54].

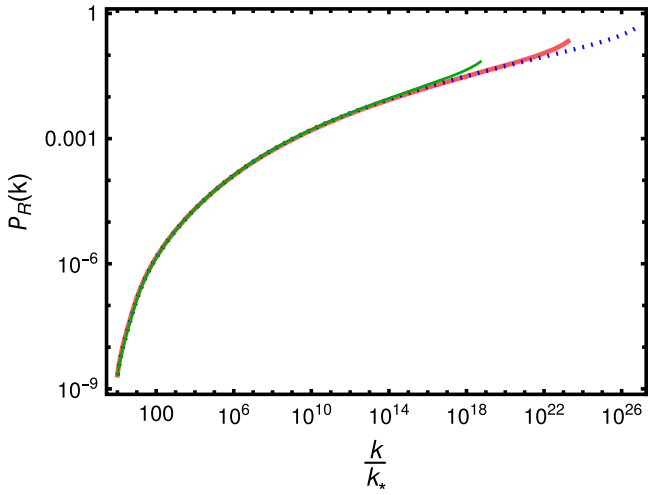

FIG. 1. Primordial power spectra generated in the WNI. The color codes are the same for the parameters as depicted in Table I.

Finally, the natural inflation potential for the inflaton field is given by [6]

$$V(\phi) = \Lambda\left(1 + \cos\left(\frac{\phi}{f}\right)\right), \tag{15}$$

where the inflaton ϕ is an "axionlike" field that is analogous to the Goldstone Boson of a broken Peccei-Quinn-like symmetry. The parameter f is the symmetry-breaking scale. This potential has been studied previously in the context of warm inflation [20–24]. In our study, we have taken $C = C_\phi/\Lambda^{1/2}$ with C_ϕ being a dimensionless model parameter, and Λ is the amplitude from Eq. (15).

The primordial curvature power spectrum for three representative sets of parameters for this model were given in Fig. 1 and are summarized here in Table I. The power spectra associated with these parameters nicely produce PBHs in the desired mass range, whereby a significant fraction (or all) of the current dark matter could be in the form of PBHs without violating observational constraints.

Since our conclusions are based upon an analysis in perturbation theory, it is important to establish that inflation terminates within the perturbative regime. In particular, the enhanced curvature perturbations must not exceed order $\mathcal{O}(1)$, above which the perturbative treatment collapses. At the same time, PBH production also requires an enhancement of the power spectrum beyond 10^{-2} to initiate a collapse. This latter requirement is due to the length scale of the fluctuations needing to be greater than the Jean's length when the associated mode reenters the horizon. It is, therefore, necessary to justify that the power spectrum will remain below the nonperturbative regime in this scenario.

TABLE I. The inflationary observable for different sets of model parameter values. The different color codes are maintained in the plots. This is the same from [1].

Color	N	$\Lambda(m_p^4)$	C_ϕ	n_s	r
Red	55	1.00×10^{-11}	50	0.964	4.0×10^{-3}
Blue	63	7.87×10^{-12}	60	0.966	4.5×10^{-4}
Green	44	1.77×10^{-11}	40	0.966	1.0×10^{-3}

To show that the nonperturbative regime is avoided, we demonstrate that inflation terminates in WNI before the perturbations exceed unity. That is, unlike cold inflation, warm inflation ends once the radiation energy density, ρ_r exceeds that of the inflation field, thus halting the growth in the power spectrum. As ρ_r becomes greater than the energy density of the inflaton, ρ_ϕ, the Universe continuously enters into the radiation-dominated era, without the need for a reheating phase.

This is depicted in Fig. 2, where for ease of comparison, we plot renormalized densities $\rho/2\Lambda$ for both the inflaton and radiation fields versus the number of e folds during inflation for each model. It is clear from this figure that the rapid falloff of ρ_ϕ for each model occurs at the number of e folds at which ρ_r becomes dominant. Thus, the power spectrum reaches its maximum right before the end of inflation while still in the perturbative regime. After the inflation ends, the perturbation modes will start reentering the horizon. All of the higher k ($k > k_{\rm eq}$) modes then reenter during radiation dominated epoch, keeping the power spectrum unchanged, such that the perturbation theory does not break down.

III. BASICS OF INDUCED GRAVITATIONAL WAVES

To model the GWs, a metric that includes both scalar and tensor perturbations is used. Within the Newtonian conformal gauge, the metric is then given by [39,42]

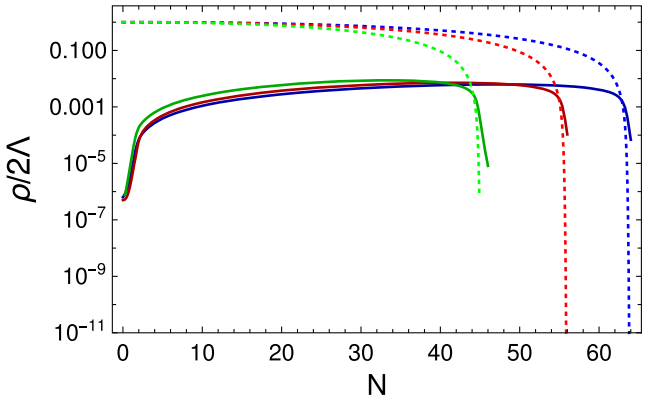

FIG. 2. Variation of normalized densities $\rho_\phi/2\Lambda$ and $\rho_r/2\Lambda$ with the number of e foldings (N). The color codes for the models are the same as depicted in Table I. Solid lines are for radiation, and the dotted lines are for the inflaton. Inflation ends once $\rho_r > \rho_\phi$ at the N quoted in Table I.

$$ds^2 = a(\eta)^2\Big[-(1+2\Phi)d\eta^2 + \left((1-2\Psi)\delta_{ij} + \frac{h_{ij}}{2}\right)dx^i dx^j\Big], \quad (16)$$

where a, is the scale factor, η is the conformal time, Φ and Ψ are the scalar perturbations, while h_{ij} is the tensor perturbation added on top of the metric. The effect of the anisotropic stress is neglected in the following discussion since its contribution is small [42]. Thus, $\Phi = \Psi$.

The action describing the tensor mode is given by

$$S = \frac{M_{\rm Pl}^2}{32}\int d\eta d^3x a^2[(h'_{ij})^2 - (\partial_l h_{ij})^2], \quad (17)$$

where the prime $'$ denotes differentiation with respect to conformal time η, while $\partial_l h_{ij}$ represents the derivative of h_{ij} with respect to spatial coordinate l.

Next the tensor perturbation can be decomposed into its Fourier modes as

$$h_{ij}(\eta, \mathbf{x}) = \int \frac{d^3k}{(2\pi)^{3/2}} \sum_{s=+,\times} \epsilon_{ij}^s(k) h_{\mathbf{k}}^s(\eta) e^{i\mathbf{kx}}, \quad (18)$$

where $\epsilon_{ij}^+(k)$ and $\epsilon_{ij}^\times(k)$ are time-independent transverse traceless polarization vectors, defined in an orthonormal basis $(e_i(\mathbf{k}), \bar{e}_i(\mathbf{k}))$ as

$$\epsilon_{ij}^+(\mathbf{k}) = \frac{1}{\sqrt{2}}[e_i(\mathbf{k})e_j(\mathbf{k}) - \bar{e}_i(\mathbf{k})\bar{e}_j(\mathbf{k})], \quad (19)$$

$$\epsilon_{ij}^\times(\mathbf{k}) = \frac{1}{\sqrt{2}}[e_i(\mathbf{k})\bar{e}_j(\mathbf{k}) + \bar{e}_i(\mathbf{k})e_j(\mathbf{k})]. \quad (20)$$

The dimensionless power spectrum for the tensor perturbation is then given by

$$\langle h_{\mathbf{k}}^\lambda(\eta) h_{\mathbf{k}'}^{\lambda'}(\eta)\rangle = \delta_{\lambda\lambda'}\frac{2\pi^2}{k^3}\delta(k+k')\mathcal{P}_h(k,\eta), \quad (21)$$

where $\lambda, \lambda' = \{+, \times\}$. What remains is to formulate equations of motion for the Fourier modes of the tensor perturbations $h_{\mathbf{k}}(\eta)$. The scalar perturbations in the gravitational potential Φ act as the source for the tensor equations of motion. Hence, following [39], we write

$$h''_{\mathbf{k}}(\eta) + 2\mathcal{H}h'_{\mathbf{k}}(\eta) + k^2 h_{\mathbf{k}}(\eta) = 4S_{\mathbf{k}}(\eta), \quad (22)$$

where the source term $S_{\mathbf{k}}$ is

$$S_{\mathbf{k}} = \int \frac{\mathrm{d}^3q}{(2\pi)^{3/2}} e_{ij}(\mathbf{k}) q_i q_j \Big(2\Phi_{\mathbf{q}}\Phi_{\mathbf{k}-\mathbf{q}} + \frac{4}{3(1+w)}(\mathcal{H}^{-1}\Phi'_{\mathbf{q}} + \Phi_{\mathbf{q}})(\mathcal{H}^{-1}\Phi'_{\mathbf{k}-\mathbf{q}} + \Phi_{\mathbf{k}-\mathbf{q}})\Big), \quad (23)$$

The above has made use of $-2\dot{H} = \rho + P = (1+w)\rho = 3(1+w)H^2$, while $w = P/\rho$ is the usual equation-of-state parameter, and $\mathcal{H} \equiv a'/a = aH$ is the Hubble parameter in conformal time. The Fourier modes of the gravitational potential $\Phi_{\mathbf{k}}$ are similar to those of the tensor mode.

Next, a Green's function method can be used to solve for $h_{\mathbf{k}}(\eta)$,

$$a(\eta)h_{\mathbf{k}}(\eta) = 4\int^\eta \mathrm{d}\bar{\eta} G_{\mathbf{k}}(\eta,\bar{\eta})a(\bar{\eta})S_{\mathbf{k}}(\bar{\eta}). \quad (24)$$

Here, the Green's function $G_{\mathbf{k}}(\eta,\bar{\eta})$ is the solution to

$$G''_{\mathbf{k}}(\eta,\bar{\eta}) + \left(k^2 - \frac{a''(\eta)}{a(\eta)}\right)G_{\mathbf{k}}(\eta,\bar{\eta}) = \delta(\eta-\bar{\eta}), \quad (25)$$

and derivatives are with respect to η.

The equation of motion for the gravitational potential (e.g., [55]) is

$$\Phi''_{\mathbf{k}} + 3\mathcal{H}(1+c_s^2)\Phi'_{\mathbf{k}} + (2\mathcal{H}' + (1+3c_s^2)\mathcal{H}^2 + c_s^2k^2)\Phi_{\mathbf{k}} = \frac{a^2}{2}\tau\delta S, \quad (26)$$

where the sound speed $c_s^2 = w$ and the temperature τ are defined via $\delta P = c_s^2\delta\rho + \tau\delta S$, and S is the entropy density. In the absence of entropy perturbations, the gravitational potential equation of motion reduces to

$$\Phi''_{\mathbf{k}}(\eta) + \frac{6(1+w)}{(1+3w)\eta}\Phi'_{\mathbf{k}}(\eta) + wk^2\Phi_{\mathbf{k}}(\eta) = 0. \quad (27)$$

The primordial value $\phi_{\mathbf{k}}$ is derived from the relation $\Phi_{\mathbf{k}} = \Phi(k\eta)\phi_{\mathbf{k}}$ where the transfer function $\Phi(k\eta)$ approaches unity well before the horizon entry. The primordial value then relates to the curvature perturbation according to

$$\langle\phi_{\mathbf{k}}\phi_{\mathbf{k}'}\rangle = \delta(\mathbf{k}+\mathbf{k}')\frac{2\pi^2}{k^3}\left(\frac{3+3w}{5+3w}\right)^2\mathcal{P}_\zeta(k), \quad (28)$$

where the EoS parameter w is evaluated before the horizon entry. The "primordial" value $\phi_{\mathbf{k}}$ is also evaluated just before the horizon entry.

The correlation function $\langle S_{\mathbf{k}}(\eta)S_{\mathbf{k}'}(\eta')\rangle$ is obtained by adopting Gaussian primordial curvature perturbations. Finally, by comparing $\langle S_{\mathbf{k}}(\eta)S_{\mathbf{k}'}(\eta')\rangle$ with $\mathcal{P}_h$, using

Eqs. (21) and (24) and doing some algebra, the power spectrum can be deduced from the curvature perturbation P_ζ [39]:

$$\mathcal{P}_h(\eta,k) = 4\int_0^\infty \mathrm{d}v \int_{|1-v|}^{1+v} \mathrm{d}u \left(\frac{4v^2-(1+v^2-u^2)^2}{4vu}\right)^2 \times I^2(v,u,x)\mathcal{P}_\zeta(kv)\mathcal{P}_\zeta(ku), \tag{29}$$

where $x \equiv k\eta$, and

$$I(v,u,x) = \int_0^x \mathrm{d}\bar{x}\frac{a(\bar{\eta})}{a(\eta)} kG_k(\eta,\bar{\eta}) f(v,u,\bar{x}), \tag{30}$$

with

$$f(v,u,\bar{x}) = \frac{6(w+1)}{3w+5}\Phi(v\bar{x})\Phi(u\bar{x}) + \frac{6(1+3w)(w+1)}{(3w+5)^2} \times (\bar{x}\partial_{\bar{\eta}}\Phi(v\bar{x})\Phi(u\bar{x}) + \bar{x}\partial_{\bar{\eta}}\Phi(u\bar{x})\Phi(v\bar{x})) + \frac{3(1+3w)^2(1+w)}{(3w+5)^2} \times \bar{x}^2\partial_{\bar{\eta}}\Phi(v\bar{x})\partial_{\bar{\eta}}\Phi(u\bar{x}), \tag{31}$$

and $\bar{x} \equiv k\bar{\eta}$, while $\mathcal{H} = aH = 2/[(1+3w)\eta]$. The function $f(u,v,\bar{x})$ contains the information about the source.

A change of variables of $u+v-1 \to t$ and $u-v \to s$ recasts the integral (29) as

$$\mathcal{P}_h(\eta,k) = 2\int_0^\infty \mathrm{d}t \int_{-1}^1 \mathrm{d}s \left(\frac{t(2+t)(s^2-1)}{(1-s+t)(1+s+t)}\right)^2 \times I^2(s,t,x)\mathcal{P}_\zeta(kv)\mathcal{P}_\zeta(ku). \tag{32}$$

For GWs produced in a radiation-dominated universe in the late time limit ($x \to \infty$), the oscillation average of $I^2(s,t,x)$ can be written as in [39],

$$\overline{I^2(s,t,x\to\infty)} = \frac{288(-5+s^2+t(2+t))^2}{x^2(1-s+t)^6(1+s+t)^6} \times \left[\frac{\pi^2}{4}(-5+s^2+t(2+t))^2\theta(t-(\sqrt{3}-1)) + (-(t-s+1)(t+s+1) + \frac{1}{2}(-5+s^2+t(2+t))\log\left|\frac{-2+t(2+t)}{3-s^2}\right|\right)\right], \tag{33}$$

where $\theta(x)$ is the Heaviside step function.

Combining Eqs. (32) and (33) and further simplifying the integral by another change of variable ($t+1 \to \sqrt{r}$), the following power spectrum is obtained:

$$\overline{\mathcal{P}_h(\eta,k)} = \int_1^\infty \mathrm{d}r \int_{-1}^1 \mathrm{d}s \frac{72(r-1)^2(s^2-1)^2(r+s^2-6)^2}{x^2\sqrt{r}(r-s^2)^8} \times \left[\left((r+s^2-6)\log\left(\left|\frac{3-r}{s^2-3}\right|\right) - 2(r-s^2)\right)^2 + \pi^2(r+s^2-6)^2\theta(\sqrt{r}-\sqrt{3})\right] \times \mathcal{P}_\zeta\left(\frac{1}{2}k(\sqrt{r}-s)\right)\mathcal{P}_\zeta\left(\frac{1}{2}k(\sqrt{r}+s)\right). \tag{34}$$

This can be numerically integrated using $\mathcal{P}_\zeta$ from Eq. (28).

IV. CONSTRAINTS ON THE GW ENERGY DENSITY

To compare WNI with GW detector sensitivities, we need to calculate the present gravitational wave closure contribution as a function of frequency. The power spectrum described in the previous section can be related directly to the energy density in gravitational waves. The GW energy density within the horizon is $\rho_{\mathrm{GW}}(\eta) = \int \mathrm{d}\ln k \rho_{\mathrm{GW}}(\eta,k)$ and can be evaluated [56] as

$$\rho_{\mathrm{GW}} = \frac{M_{\mathrm{Pl}}^2}{16a^2}\langle\overline{h_{ij,k}h_{ij,k}}\rangle, \tag{35}$$

where the overline indicates an average over the oscillations. We have considered the parity invariance for the polarization modes such that both have the same contribution to the energy density. The fraction of the GW energy density per logarithmic wave number, $\Omega_{\mathrm{GW}}(\eta,k)$ is then given by:

$$\Omega_{\mathrm{GW}}(\eta,k) = \frac{1}{\rho_{\mathrm{tot}}(\eta)}\frac{d\rho_{\mathrm{GW}}(\eta,k)}{d\ln k} = \frac{\rho_{\mathrm{GW}}(\eta,k)}{\rho_{\mathrm{tot}}(\eta)} = \frac{1}{24}\left(\frac{k}{a(\eta)H(\eta)}\right)^2\overline{\mathcal{P}_h(\eta,k)}, \tag{36}$$

where a sum has been made over the two polarization modes. During the radiation-dominated era, the term in parentheses simplifies to

$$\left(\frac{k}{a(\eta)H(\eta)}\right)^2 = k^2\eta^2 = x^2. \tag{37}$$

To obtain the present spectrum of gravitational waves from Eq. (37) following [39], we deduce (see Appendix)

$$\Omega_{\mathrm{GW},0}(k) = 0.39\left(\frac{g_*(T_c)}{106.75}\right)^{-1/3}\Omega_{r,0}\,\Omega_{\mathrm{GW}}(\eta_c, k), \quad (38)$$

where the subscript (c) denotes quantities evaluated when the perturbation is within the horizon during the radiation-dominated era when ρ_{GW} is a constant fraction of the radiation energy density. We use $\Omega_{r,0}h^2$ $(=4.18\times10^{-5})$ for the present closure contribution from photons and neutrinos. Finally, the wave number k is related to the frequency of gravitational waves by

$$f = \frac{k}{2\pi} = 1.5\times10^{-15}\left(\frac{k}{1\ \mathrm{Mpc}^{-1}}\right)\ \mathrm{Hz}. \quad (39)$$

Figure 3 shows the present gravitational closure contribution as a function of frequency. The continuous green, red, and blue lines show calculated contribution in gravitational radiation $\Omega_{\mathrm{GW}}h^2$ from primordial black holes for $N = 44$, 55, 63 e folds of inflation, respectively. Note the sharp dropoff in the power once the scale of PBH formation is obtained.

Various lines on Fig. 3 indicate current (blue lines) and anticipated future (pink lines) constraints from various GW observatories as labeled. The jagged blue lines indicate existing pulsar timing array constraints from EPTA [57], NANOGrav [58], and PPTA [59]. The horizontal blue dashed line shows the BBN upper bound on the energy density in gravitational waves, $\Omega_{\mathrm{GW}}h^2 < 1.8\times10^{-6}$ (95% C.L.) deduced in [39].

The pink lines show sensitivity curves [60] of various future GW observations reproduced from Ref. [61]. The curves are from SKA [62], eLISA [63], LISA [64], BBO [65], DECIGO [66], Einstein Telescope [67], Cosmic Explorer [68], and KAGRA [69].

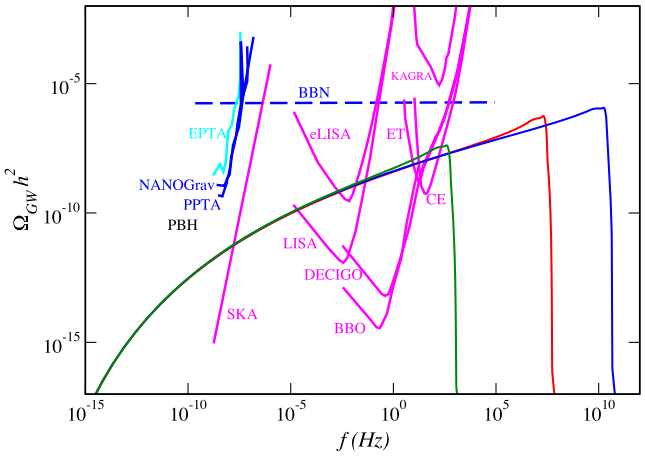

FIG. 3. Green, red, and blue solid lines show calculated closure contribution in gravitational radiation $\Omega_{\mathrm{GW}}h^2$ from primordial black holes in WNI for $N = 44$, 55, 60 e folds of inflation. These are compared with various constraints as labeled. Blue colors denote existing constraints from pulsar timing and BBN, while pink colors show constraints from future space-based and ground-based GW observatories.

As seen from this figure, the predicted contribution from PBH GWs easily satisfies current constraints from pulsar timing and BBN. Perhaps, more interesting is the fact that pending space-based detectors such as LISA, BBO, and DECIGO will have sufficient sensitivity to detect this contribution from PBH gravitational waves. Even next-generation ground-based detectors like the Einstein Telescope and the Compton Explorer may get a glimpse of this possible GW background.

V. CONCLUSION

We have calculated the contribution to the closure density $\Omega_{\mathrm{GW}}h^2$ from the energy density in gravitational waves for models of warm natural inflation that produce PBHs in a mass range that could account for as much as all of the presently inferred dark matter. The case of PBHs in cold inflation has been studied extensively in the recent literature (e.g., Refs. [70–74]). However, we have shown in particular that the contribution of Ω_{GW} from WNI satisfies all existing constraints from BBN and pulsar timing. Moreover, we show the interesting result that this cosmic background in GWs may be detectable in the next generation of space-based and ground-based gravitational wave interferometers.

The observation of GWs predicted by this model could point toward indirect evidence of the warm inflationary paradigm. Of course, one should also explore many avenues to check the shape of the secondary GWs produced due to the enhancement in the primary scalar power spectrum. For example, one interesting aspect that one can check is the effect on the GW spectrum in the case of resonant particle production during inflation as described in [75,76].

Also, a more general form of pseudo-Nambu Goldstone Boson(pNGB) inflaton has been studied in [77] and studied in alternative scenarios in [78–81]. This has been dubbed as Goldstone inflation. In this case, natural inflation is just a limiting case of the more general Goldstone inflation. It will be of interest to study this more general model in the context of the WI and study further the PBH production and GW production associated with it.

Furthermore, a reconstruction of the inflationary potential in the WI paradigm while keeping the PBH production in mind to account for the total DM density could lead to interesting results as in the case of [82].

Finally, we note a recent suggestion that the production of PBHs faces a no-go theorem in the case of single-field cold inflation [83]. We emphasize, however, that the production of PBHs and consequently GWs in the context of WNI as discussed here is both allowed and quite inevitable. Thus, testing this theory following the path of [83–88] (though there are counterarguments presented in [89]) could

lead to interesting insight into the physics of the early inflationary universe. The authors plan to consider these in future work.

ACKNOWLEDGMENTS

The authors would like to thank M. Sami and Yogesh for the useful discussions. N. J. is thankful to Sirshendu for his help. Work at the University of Notre Dame supported by DOE nuclear theory Grant No. DE-FG02-95-ER40934. Work of M. R. G. is supported by DST, Government of India under the Grant Agreement No. IF18-PH-228 and by Science and Engineering Research Board (SERB), DST, Government of India under the Grant Agreement No. CRG/2022/004120 (Core Research Grant). N. J. is supported by the National Postdoctoral Fellowship of the Science and Engineering Research Board (SERB), Department of Science and Technology (DST), Government of India, File No. PDF/2021/004114.

APPENDIX

Here we show the derivation of $\Omega_{\rm GW}$. Following [39], we write

$$\Omega_{\rm GW,0}(k) = \frac{\rho_{\rm GW}(\eta_0,k)}{\rho_{\rm tot}(\eta_0)} = \frac{\rho_{\rm GW}(\eta_0,k)}{\rho_{\rm GW}(\eta_c,k)}\frac{\rho_{\rm GW}(\eta_c,k)}{\rho_{\rm tot}(\eta_0)} = \frac{\rho_{\rm GW}(\eta_0,k)}{\rho_{\rm GW}(\eta_c,k)}\frac{\rho_{\rm GW}(\eta_c,k)}{\rho_{\rm tot}(\eta_c)}\frac{\rho_{\rm tot}(\eta_c)}{\rho_{\rm tot}(\eta_0)}. \tag{A1}$$

During the radiation dominated era, $\rho_{\rm tot}(\eta_c) \approx \rho_r(\eta_c)$ and also $\rho_{\rm GW} \sim a^{-4}$. Thus, can we write

$$= \frac{a(\eta_c)^4}{a(\eta_0)^4}\Omega_{\rm GW}(\eta_c,k)\frac{\rho_r(\eta_c)}{\rho_{\rm tot}(\eta_0)} \tag{A2}$$

$$= \frac{a(\eta_c)^4}{a(\eta_0)^4}\Omega_{\rm GW}(\eta_c,k)\frac{\rho_r(\eta_0)}{\rho_{\rm tot}(\eta_0)}\frac{\rho_r(\eta_c)}{\rho_r(\eta_0)} \tag{A3}$$

$$= \frac{a(\eta_c)^4}{a(\eta_0)^4}\Omega_{\rm GW}(\eta_c,k)\Omega_{r,0}\frac{\rho_r(\eta_c)}{\rho_r(\eta_0)}. \tag{A4}$$

Now, from the conservation of entropy we get

$$\frac{\rho_r(\eta_c)}{\rho_r(\eta_0)} = \frac{g_{*,c}}{g_{*,0}}\left(\frac{T_c}{T_0}\right)^4 \tag{A5}$$

$$= \frac{g_{*,c}}{g_{*,0}}\left(\frac{g_{*S,0}}{g_{*S,c}}\right)^{4/3}\frac{a(\eta_0)^4}{a(\eta_c)^4}, \tag{A6}$$

where $g_{*,c}$ is the number of relativistic degrees freedom at temperature T_c; similarly g_{*S} is the same for entropy density. Before $e^+ - e^-$ pair annihilation during the radiation era, $g_{*S,c} \approx g_{*,c}$, Thus, we deduce

$$\Omega_{\rm GW,0}(k) = \left(\frac{g_{*,c}}{g_{*,0}}\right)\left(\frac{g_{*S,0}}{g_{*S,c}}\right)^{4/3}\Omega_{r,0}\,\Omega_{\rm GW} = 0.39\left(\frac{g_{*,c}}{106.75}\right)^{-1/3}\Omega_{r,0}\,\Omega_{\rm GW}(\eta_c,k), \tag{A7}$$

where, the latter equation makes use of standard values $g_{*,0} = 3.36$ and $g_{*S,0} = 3.91$, and 106.75 is the number of degrees of freedom from standard-model particles.

[1] M. Correa, M. R. Gangopadhyay, N. Jaman, and G. J. Mathews, Phys. Lett. B **835**, 137510 (2022).
[2] A. H. Guth, Phys. Rev. D **23**, 347 (1981).
[3] A. D. Linde, Phys. Lett. **129B**, 177 (1983).
[4] V. F. Mukhanov, H. A. Feldman, and R. H. Brandenberger, Phys. Rep. **215**, 203 (1992).
[5] A. A. Starobinsky, Phys. Lett. **91B**, 99 (1980).
[6] K. Freese, J. A. Frieman, and A. V. Olinto, Phys. Rev. Lett. **65**, 3233 (1990).
[7] A. Berera and L.-Z. Fang, Phys. Rev. Lett. **74**, 1912 (1995).
[8] A. Berera, Phys. Rev. Lett. **75**, 3218 (1995).
[9] M. Bastero-Gil, A. Berera, R. O. Ramos, and J. G. Rosa, Phys. Rev. Lett. **117**, 151301 (2016).
[10] R. O. Ramos and L. A. da Silva, J. Cosmol. Astropart. Phys. 03 (2013) 032.
[11] M. Bastero-Gil, A. Berera, I. G. Moss, and R. O. Ramos, J. Cosmol. Astropart. Phys. 05 (**2014**) 004.
[12] M. Bastero-Gil, S. Bhattacharya, K. Dutta, and M. R. Gangopadhyay, J. Cosmol. Astropart. Phys. 02 (2018) 054.
[13] M. Bastero-Gil, A. Berera, and R. O. Ramos, J. Cosmol. Astropart. Phys. 09 (2011) 033.
[14] I. G. Moss and C. Xiong, arXiv:hep-ph/0603266.
[15] A. Berera, M. Gleiser, and R. O. Ramos, Phys. Rev. D **58**, 123508 (1998).
[16] M. Bastero-Gil, A. Berera, and N. Kronberg, J. Cosmol. Astropart. Phys. 12 (2015) 046.
[17] M. Bastero-Gil, A. Berera, and J. R. Calderón, J. Cosmol. Astropart. Phys. 07 (2019) 019.
[18] S. Basak, S. Bhattacharya, M. R. Gangopadhyay, N. Jaman, R. Rangarajan, and M. Sami, J. Cosmol. Astropart. Phys. 03 (2022) 063.
[19] R. D'Agostino and O. Luongo, Phys. Lett. B **829**, 137070 (2022).
[20] H. Mishra, S. Mohanty, and A. Nautiyal, Phys. Lett. B **710**, 245 (2012).
[21] L. Visinelli, J. Cosmol. Astropart. Phys. 09 (2011) 013.
[22] Y. Reyimuaji and X. Zhang, J. Cosmol. Astropart. Phys. 04 (2021) 077.

[23] G. Montefalcone, V. Aragam, L. Visinelli, and K. Freese, J. Cosmol. Astropart. Phys. 03 (**2023**) 002.
[24] M. AlHallak, K. K. A. Said, N. Chamoun, and M. S. El-Daher, Universe **9**, 80 (2023).
[25] P. A. R. Ade *et al.* (Planck Collaboration), Astron. Astrophys. **594**, A13 (2016); arXiv:1502.02114.
[26] N. Aghnim *et al.* (Planck Collaboration), Astron. Astrophys. **641**, A6 (2020).
[27] P. A. R. Ade *et al.* (Keck Array and BICEP2 Collaborations), Phys. Rev. Lett. **116**, 031302 (2016).
[28] P. A. R. Ade *et al.*, Phys. Rev. Lett. **114**, 101301 (2015).
[29] Y. B. Zel'dovich and I. D. Novikov, Sov. Astron. AJ (Engl. Transl.), **10**, 602 (1967).
[30] S. Hawking, Mon. Not. R. Astron. Soc. **152**, 75 (1971).
[31] B. J. Carr and S. W. Hawking, Mon. Not. R. Astron. Soc. **168**, 399 (1974).
[32] G. F. Chapline, Nature (London) **253**, 251 (1975).
[33] B. Carr, F. Kuhnel, and M. Sandstad, Phys. Rev. D **94**, 083504 (2016).
[34] B. Carr and F. Kuhnel, Annu. Rev. Nucl. Part. Sci. **70**, 355 (2020).
[35] G. Ballesteros and M. Taoso, Phys. Rev. D **97**, 023501 (2018).
[36] R. Arya, J. Cosmol. Astropart. Phys. 09 (2020) 042.
[37] N. Cappelluti, G. Hasinger, and P. Natarajan, Astrophys. J. **926**, 205 (2022).
[38] R. P. Naidu *et al.*, Astrophys. J. Lett. **940**, L14 (2022).
[39] K. Kohri and T. Terada, Phys. Rev. D **97**, 123532 (2018).
[40] K. N. Ananda, C. Clarkson, and D. Wands, Phys. Rev. D **75**, 123518 (2007).
[41] S. Mollerach, D. Harari, and S. Matarrese, Phys. Rev. D **69**, 063002 (2004).
[42] D. Baumann, P. J. Steinhardt, K. Takahashi, and K. Ichiki, Phys. Rev. D **76**, 084019 (2007).
[43] S. Choudhury and A. Mazumdar, Phys. Lett. B **733**, 270 (2014).
[44] G. Domènech, Universe **7**, 398 (2021).
[45] G. Domènech, Int. J. Mod. Phys. D **29**, 2050028 (2020).
[46] G. Domènech, S. Pi, and M. Sasaki, J. Cosmol. Astropart. Phys. 08 (2020) 017.
[47] E. Bugaev and P. Klimai, Phys. Rev. D **81**, 023517 (2010).
[48] L. Alabidi, K. Kohri, M. Sasaki, and Y. Sendouda, J. Cosmol. Astropart. Phys. 09 (**2012**) 017.
[49] M. Bastero-Gil and M. S. Díaz-Blanco, J. Cosmol. Astropart. Phys. 12 (2021) 052.
[50] M. R. Gangopadhyay, S. Myrzakul, M. Sami, and M. K. Sharma, Phys. Rev. D **103**, 043505 (2021).
[51] R. Arya and A. K. Mishra, Phys. Dark Universe **37**, 101116 (2022).
[52] R. Arya, R. K. Jain, and A. K. Mishra, arXiv:2302.08940.
[53] S. Bartrum, M. Bastero-Gil, A. Berera, R. Cerezo, R. O. Ramos, and J. G. Rosa, Phys. Lett. B **732**, 116 (2014).
[54] M. Benetti and R. O. Ramos, Phys. Rev. D **95**, 023517 (2017).
[55] V. Mukhanov, *Physical Foundations of Cosmology* (Cambridge University Press, Oxford, 2005).
[56] M. Maggiore, Phys. Rep. **331**, 283 (2000).
[57] L. Lentati *et al.*, Mon. Not. R. Astron. Soc. **453**, 2576 (2015).
[58] Z. Arzoumanian *et al.* (NANOGrav Collaboration), Astrophys. J. **859**, 47 (2018).
[59] R. M. Shannon *et al.*, Science **349**, 1522 (2015).
[60] B. S. Sathyaprakash and B. F. Schutz, Living Rev. Relativity **12**, 2 (2009).
[61] C. J. Moore, R. H. Cole, and C. P. L. Berry, Classical Quantum Gravity **32**, 015014 (2015).
[62] P. E. Dewdney, P. J. Hall, R. T. Schilizzi, and T. J. L. W. Lazio, Proc. IEEE **97**, 1482 (2009).
[63] P. A. Seoane *et al.* (eLISA Collaboration), arXiv:1305.5720.
[64] P. Amaro-Seoane *et al.* (LISA Collaboration), arXiv:1702.00786.
[65] G. M. Harry, P. Fritschel, D. A. Shaddock, W. Folkner, and E. S. Phinney, Classical Quantum Gravity **23**, 4887 (2006); **23**, 7361(E) (2006).
[66] N. Seto, S. Kawamura, and T. Nakamura, Phys. Rev. Lett. **87**, 221103 (2001).
[67] M. Punturo *et al.*, Classical Quantum Gravity **27**, 194002 (2010).
[68] B. P. Abbott *et al.* (LIGO Scientific Collaboration), Classical Quantum Gravity **34**, 044001 (2017).
[69] K. Somiya for the KAGRA Collaboration, Classical Quantum Gravity **29**, 124007 (2012).
[70] M. Sasaki, T. Suyama, T. Tanaka, and S. Yokoyama, Classical Quantum Gravity **35**, 063001 (2018).
[71] K. Inomata, M. Kawasaki, K. Mukaida, Y. Tada, and T. T. Yanagida, Phys. Rev. D **96**, 043504 (2017).
[72] S. S. Mishra and V. Sahni, J. Cosmol. Astropart. Phys. 04 (2020) 007.
[73] S. Bhattacharya, A. Das, and K. Dutta, J. Cosmol. Astropart. Phys. 10 (2021) 071.
[74] R. Zheng, J. Shi, and T. Qiu, Chin. Phys. C **46**, 045103 (2022).
[75] G. J. Mathews, M. R. Gangopadhyay, K. Ichiki, and T. Kajino, Phys. Rev. D **92**, 123519 (2015).
[76] M. R. Gangopadhyay, G. J. Mathews, K. Ichiki, and T. Kajino, Eur. Phys. J. C **78**, 733 (2018).
[77] D. Croon, V. Sanz, and J. Setford, J. High Energy Phys. 10 (2015) 020.
[78] S. Bhattacharya and M. R. Gangopadhyay, Phys. Rev. D **101**, 023509 (2020).
[79] H. A. Khan and Yogesh, Phys. Rev. D **105**, 063526 (2022).
[80] M. R. Gangopadhyay, H. A. Khan, and Yogesh, Phys. Dark Universe **40**, 101177 (2023).
[81] M. R. Gangopadhyay, N. Kumar, A. Mukherjee, and M. K. Sharma, arXiv:2205.15249.
[82] S. Bhattacharya, K. Das, and M. R. Gangopadhyay, Classical Quantum Gravity **37**, 215009 (2020).
[83] S. Choudhury, M. R. Gangopadhyay, and M. Sami, arXiv:2301.10000.
[84] S. Choudhury, S. Panda, and M. Sami, Phys. Lett. B **845**, 138123 (2023).
[85] S. Choudhury, S. Panda, and M. Sami, J. Cosmol. Astropart. Phys. 11 (2023) 066.
[86] S. Choudhury, S. Panda, and M. Sami, J. Cosmol. Astropart. Phys. 08 (2023) 078.
[87] J. Kristiano and J. Yokoyama, arXiv:2211.03395.
[88] J. Kristiano and J. Yokoyama, arXiv:2303.00341.
[89] A. Riotto, arXiv:2301.00599.